

Effects of Variant Positions of Cold Walls on Natural Convection in a Triangular Cavity

M. Triveni[†], R. Panua and D. Sen

Department of Mechanical Engineering, National Institute of Technology Agartala, Tripura, 799055

[†]Corresponding Author Email:triveni_mikky@yahoo.com

(Received August 25, 2014; accepted November 10, 2014)

ABSTRACT

The effect of different configurations of partial cold walls on laminar natural convection heat transfer for a right-angle triangular cavity heated from below has been studied numerically. The enclosure is filled with water and heat transfer surfaces such as hot and cold walls are maintained at constant temperature. The side and hypotenuse walls of the enclosure are detached from the middle and have been arranged in four different configurations, namely AB, BC, AD and CD for cooling purpose. The finite volume method is used to solve the dimensionless governing mass, momentum and energy equations. The problem has been solved to explore the effects of the pertinent parameters i.e. different configurations of cold walls and variation of Rayleigh number ($10^5 \leq Ra \leq 10^7$). Results are obtained from numerical simulation using commercial software package, FLUENT and presented in the form of streamlines and isotherms. The thermal performance of the enclosure has been expressed by local and average Nusselt numbers. From the analysis, it is observed that the temperature distribution and flow field are significantly affected by these parameters. The high heat transfer rate has been observed for the position AB while low for the position CD. Also, the heat transfer rate enhances as the Rayleigh number (Ra) increases.

Keywords: Cold walls positions; Natural convection; Triangular enclosure; Rayleigh number.

NOMENCLATURE

b	width of the cavity	x, y	co-ordinates
g	acceleration due to gravity	X, Y	dimensionless co-ordinates
h	hypotenuse of the cavity	α	thermal diffusivity
H	height of the cavity	β	thermal expansion coefficient
Nux	local Nusselt number	θ	dimensionless temperature
Nu	average nusselt number	k	thermal conductivity
p	pressure	ρ	density
P	dimensionless pressure	μ	dynamic viscosity
Pr	Prandtl number	ν	kinematic viscosity
Ra	Rayleigh number	ψ	stream function
T	temperature	Ψ	dimensionless stream function
T_c	cold wall temperature		
T_h	hot wall temperature		
U, V	dimensionless velocity components		
u, v	velocity components		

Subscripts

h	hot wall
c	cold wall

1. INTRODUCTION

A lot of work has been conducted on Natural convection heat transfer in fluid-filled enclosures using square, rectangular, rhombus, triangular enclosures, experimentally or numerically or both, due to its wide applications in cooling of electronic equipments, heating and cooling of building, solar collectors, geophysical

field etc. But the free convection heat transfer in triangular enclosure heating from below is substantially related to building attics and cooling of electronic equipments(Varol *et al.* 2008). Flack *et al.* (1979, 1980) were the first researchers who investigated natural convection heat transfer on triangular enclosure. After that so many studies have been carried out in triangular enclosures. Akinsete and Coleman (1982) performed a heat

transfer analysis on pitched roofs with horizontal suspended ceiling in a horizontal right-angled triangular cavity. Results reported that the heat transfer across the base wall increases towards the hypotenuse/base wall intersection. Asan and Namli (2000) have executed a numerical study for laminar natural convection in a pitched roof cross section under summer day boundary conditions. Problem was solved for different height – base ratio and Rayleigh number range, $\text{Ra} = 10^3\text{--}10^6$. Ridouane et al.(2005) have numerically computed laminar natural convection in a right-angled triangular cavity filled with air. The study reported that this work might find the application in electronic equipment's. From the investigation it was examined that the heat transfer enhancement gets decreased when both apex angle and Rayleigh number reduces. Tzeng et al.(2005) proposed a numerical simulation aided parametric analysis to solve the natural convection equations in streamline-vorticity form. Varol et al.(2007) have done a numerical analysis in triangular enclosure with heater. The problem has been solved for different Rayleigh number, aspect ratio, height, width and location of heater. Results were concluded that, for high heat transfer rate, heater must be located at the center of the bottom wall and aspect ratio and height of the heater should be high. Koca et al. (2007) have investigated a computational work in triangular enclosure with localized heating from below. Computations were carried out for dimensionless heater locations ($0.15 \leq s \leq 0.95$), dimensionless heater length ($0.1 \leq w \leq 0.9$), Prandtl number ($0.01 \leq \text{Pr} \leq 15$) and Rayleigh number ($10^3 \leq \text{Ra} \leq 10^6$). The results have drawn out from the analysis that the heat transfer increases with the increase of heater length and Ra. Varol et al. (2007) attached a thin solid adiabatic fin in a porous right-angled triangular enclosure and solved numerically using finite volume method. They found that the Nusselt number is an increasing function of Rayleigh number and with the increasing dimensionless solid adiabatic fin height, the heat transfer rate decreases. Varol et al. (2008) solved natural convection heat transfer numerically in a triangular enclosure filled with porous media and heated non-isothermally from the bottom wall. It was observed that the heat transfer enhancement is found when vertical and inclined walls are isothermal and bottom wall is at non-uniform temperature. Varol et al. (2008) performed a numerical investigation of entropy generation due to partially heating in isosceles triangular enclosure. It was stated that the entropy production number increases but Bejan number decreases with the increase of Rayleigh number. Also, the Nusselt number increases with increasing Rayleigh number and length of the heater. Kent (2009) has conceded a numerical analysis in isosceles triangular enclosure for cold base and hot inclined walls. The base angles were varied from 15° to 17° and Rayleigh number ($10^3 \leq \text{Ra} \leq 10^5$). The investigation reported that the enclosure with low aspect ratio have higher heat transfer rate from bottom surface of the triangular cavity. Basak et al. (2009) used a triangular cavity for heat transfer. It was found that the heatlines are conduction

dominant at low Rayleigh number while convection dominant for high Rayleigh number. Kaluri et al.(2010) have solved a natural convection in right-angled triangular enclosure with various top angles and different thermal boundary conditions for $\text{Ra} = 10^3\text{--}10^5$ via heat flow analysis. They reported that the uniform heating cases exhibit high heat transfer rate than linear heating cases. Xu et al. (2010) carried out a steady-state laminar natural convection heat transfer around a horizontal cylinder in a concentric triangular enclosure. They informed that the flow intensity and overall heat transfer are significantly enhancing with Rayleigh number. S.C. Saha (2011) has examined heat transfer and fluid flow in a triangular enclosure with instantaneous heating on the inclined walls. It was noticed that initially the Nusselt number was very high due to conduction effect and after that it decreases gradually and become steady state. Rahman et al. (2012)examined the effects of buoyancy ratio (Br) and Lewis number (Le) on heat transfer in a triangular cavity with zigzag shaped bottom wall. They observed that the average Nu increases with increase of Br while it decreases with the increase of Le. However, Sherwood number is increasing with the increase of both Br and Le. Basak et al. (2012) worked in entropy generation due to natural convection in right-angled triangular enclosures filled with porous media. It has been observed that the total entropy generation increases with the increase in Darcy number. Bose et al. (2012) performed a numerical work on quadrantal cavity heating from side wall using adiabatic fin and cooled from the base wall. From the investigation it was summarized that the using an adiabatic fin on hot wall enhances the flow strength and heat transfer increases with the increase of Rayleigh number. Walid and Ahmed (2012) have done a numerical analysis on prismatic cavity for fluid flow and heat transfer. The result reported that the heat transfer is affected by aspect ratio and it increases with the increase of Rayleigh number. Pullepu and Chamka (2012) investigated the unsteady laminar natural convection in a vertical cone, using non-uniform surface heat flux. Results unfold that the values of local and average Nusselt number reduce with the increase of cone angle (ϕ) or decrease in Pr. Yesiloz and Aydin (2013)have executed the experimental and numerical work in right-angled triangular cavity heated from below and cooled from the side wall. They introduce a new approach to overcome the singularity at the corner joining. The result concludes that the heat transfer rate increases with the increase in Rayleigh number. Bhardwaj and Dalal (2013)reported a numerical investigation of two-dimensional porous right-angled triangular enclosure. It was observed that the heat transfer increases with the increase in Darcy number.

The above brief literature survey reported that the most of the appraisals have been carried out on the triangular cavities heating from below and cooling by either side or hypotenuse wall or using both walls. But no study has yet been executed on

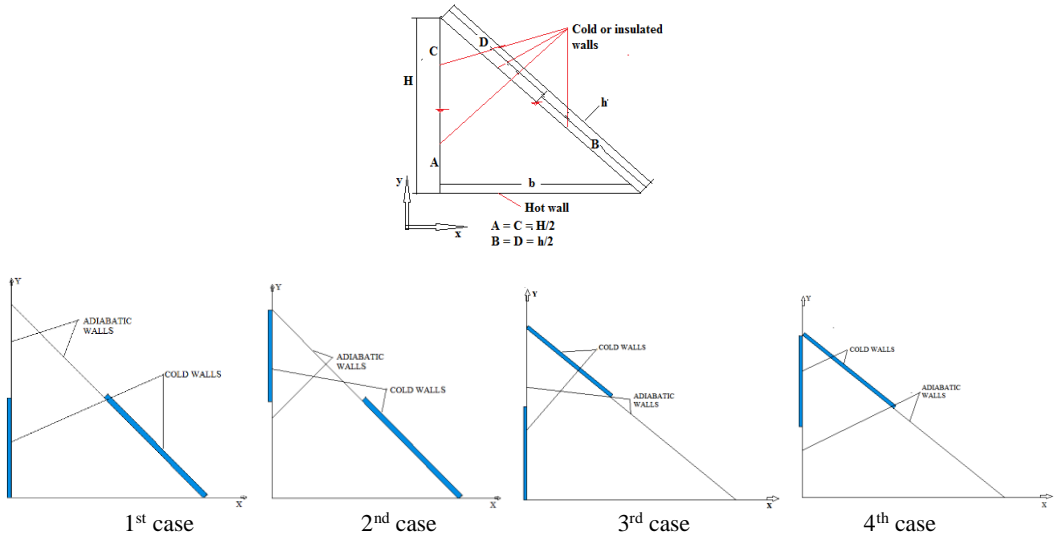


Fig. 1. Physical model and boundary conditions for triangular cavity.

triangular cavity heating from below, cooling from both halves of the side and hypotenuse walls and simultaneously, other halves are kept insulated. Hence, the main aim of this study is to investigate the effect of various configurations of cooling walls and Rayleigh number on the heat transfer in a right-angled triangular cavity. Indeed, this study has the potential application in cooling of electronic devices where the complete wall (side and hypotenuse) of the enclosure is not allowed for cooling but a part of it is permissible due to the geometric constrain.

2. PROBLEM DEPICTION AND MATHEMATICAL FORMULATION

The 2D right-angled triangular cavity of base b , height H and hypotenuse h is shown in Fig. 1 along with the confined boundary conditions. The side and inclined walls are divided from the middle ($A = C = H/2$ and $B = D = h/2$) and configured in four different ways namely AB, AD, BC & CD. The base wall of the enclosure is considered as hot wall and maintained at constant temperature T_h whereas the partitioned walls are considered as cold (T_c) and adiabatic wall. Copper is used for active thermal walls while Plexiglas as an insulating material for adiabatic walls. The cavity is filled with water which disperses inside the cavity by virtue of temperature difference. The following assumptions have been made for a steady laminar flow inside a triangular cavity which is as follows:

- All walls are impermeable.
- Radiation effect is negligible.
- The fluid is incompressible.
- No external agency has been used for fluid flow.
- The variation in fluid properties with temperature is negligible except the density variation in the body force term.

Based on the above assumptions, the non-dimensional governing equations can be written by using the dimensionless parameters

$$\begin{aligned} X &= \frac{x}{H}, Y = \frac{y}{H}, U = \frac{uH}{\alpha}, V = \frac{vH}{\alpha}, \theta = \frac{T - T_c}{T_h - T_c}, \\ P &= \frac{pH^2}{\rho\alpha^2}, \text{Pr} = \frac{\nu}{\alpha}, Ra = \frac{g\beta(T_h - T_c)H^3}{\alpha\nu} \end{aligned} \quad (1)$$

as:

$$\frac{\partial U}{\partial X} + \frac{\partial V}{\partial Y} = 0 \quad (2)$$

$$U \frac{\partial U}{\partial X} + V \frac{\partial U}{\partial Y} = -\frac{\partial P}{\partial X} + \text{Pr} \left(\frac{\partial^2 U}{\partial X^2} + \frac{\partial^2 U}{\partial Y^2} \right) \quad (3)$$

$$U \frac{\partial V}{\partial X} + V \frac{\partial V}{\partial Y} = -\frac{\partial P}{\partial Y} + \text{Pr} \left(\frac{\partial^2 V}{\partial X^2} + \frac{\partial^2 V}{\partial Y^2} \right) + Ra \text{Pr} \theta \quad (4)$$

$$U \frac{\partial \theta}{\partial X} + V \frac{\partial \theta}{\partial Y} = \left(\frac{\partial^2 \theta}{\partial X^2} + \frac{\partial^2 \theta}{\partial Y^2} \right) \quad (5)$$

and dimensionless boundary conditions are as follows:

Hot wall:

$$\theta = 1, U = V = 0 \text{ at } Y = 0, 0 \leq X \leq 1$$

Cold wall:

At the lower half of the side wall:

$$\theta = 0, U = V = 0 \text{ for } X = 0 \text{ and } 0 \leq Y \leq 1/2 \quad (6)$$

At the upper half of the side wall:

$$\theta = 0, U = V = 0 \text{ for } X = 0, 1/2 \leq Y \leq 1$$

At the upper half of the hypotenuse wall

$$\theta = 0, U = V = 0 \text{ for } 0 \leq X \leq 1/2 \text{ and } 1/2 \leq Y \leq 1$$

At the lower half of the hypotenuse wall

$$\theta = 0, U = V = 0 \text{ for } 1/2 \leq X \leq 1 \text{ and } 0 \leq Y \leq 1/2$$

Adiabatic wall

At the lower half of the side wall:

$$\frac{\partial \theta}{\partial n} = 0, U = V = 0 \text{ for } X = 0, 0 \leq Y \leq 1/2$$

At the upper half of the side wall:

$$\frac{\partial \theta}{\partial n} = 0, U = V = 0 \text{ for } X = 0, 1/2 \leq Y \leq 1$$

At the upper half of the hypotenuse wall

$$\frac{\partial \theta}{\partial n} = 0, U = V = 0 \text{ for } 0 \leq X \leq 1/2 \text{ and } 1/2 \leq Y \leq 1$$

At the lower half of the hypotenuse wall

$$\frac{\partial \theta}{\partial n} = 0, U = V = 0 \text{ for } 1/2 \leq X \leq 1 \text{ and } 0 \leq Y \leq 1/2$$

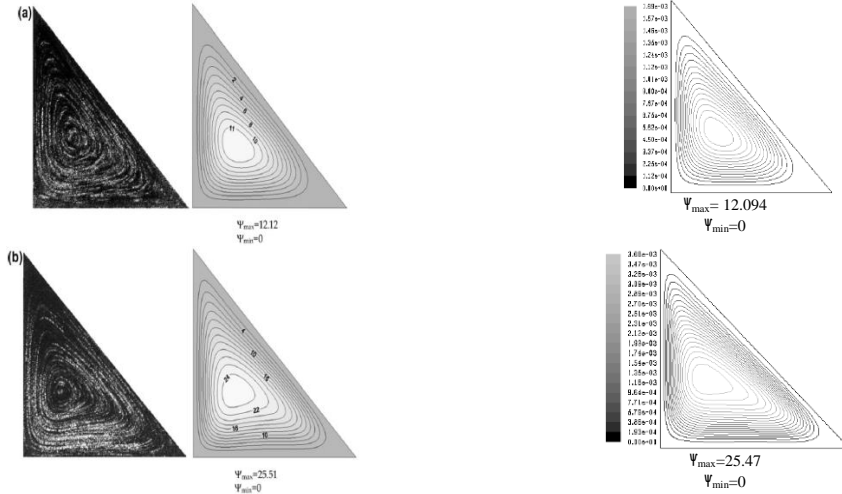


Fig. 3. Comparison of streamlines between the present results (right) and the experimental and numerical results (left) of Yesiloz&Aydin for a) $\text{Ra} = 10^5$ and b) $\text{Ra} = 5 \times 10^5$.

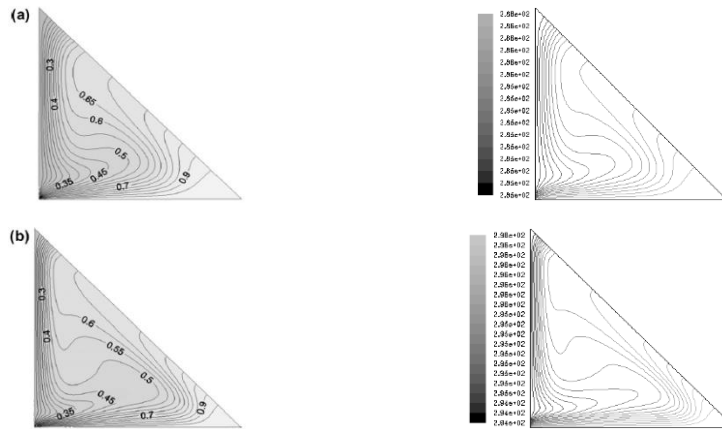


Fig. 4. Comparison of isotherms between the present results (right) and the experimental and numerical results (left) of Yesiloz & Aydin for a) $\text{Ra} = 10^5$ and b) $\text{Ra} = 5 \times 10^5$.

3. NUMERICAL METHODOLOGY

The commercially available software FLUENT 6.3 is used to solve this problem numerically. The governing equations (2-5) with the corresponding boundary conditions (6) are solved by the control volume formulation using SIMPLE algorithm. The local Nusselt number is calculated by standard definition of Nusselt number ($\text{Nu}_x = hL/k$) while the average Nusselt number is calculated through new definition of average Nusselt number ($\text{Nu} = \frac{dT}{d\phi} \Big|_{\phi=0} \frac{1}{T_h - T_c} \frac{\pi}{2}$) introduced by Yesiloz and Aydin (2013) to overcome the singularity problem in a triangular cavity.

The stream function is defined as

$$u = \frac{\partial \psi}{\partial y}, v = -\frac{\partial \psi}{\partial x} \quad (7)$$

And the non-dimensional stream function has been calculate by

$$\Psi = \psi/\alpha \quad (8)$$

3.1 Grid Independency Test

The detailed grid independency test has been conducted for the recommended mesh structure,

shown in Fig.2, for six different mesh sizes such as 60×60 , 80×80 , 100×100 , 120×120 , 140×140 and 160×160 . The independency on grid has been considered on the basis of less deviation in non-dimensional stream function (Ψ) and average Nusselt number (Nu) which was calculated by relative error analysis. The less deviation in Ψ and Nu has been found between 100×100 and 120×120 which is manifested in Table 1. Hence, 14400 grids are recommended for better accuracy and less convergence time to the problem.

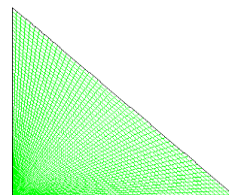


Fig. 2. Recommended grid structures for present investigation.

3.2 Validation

The simulated results have been validated with the published experimental and numerical results of

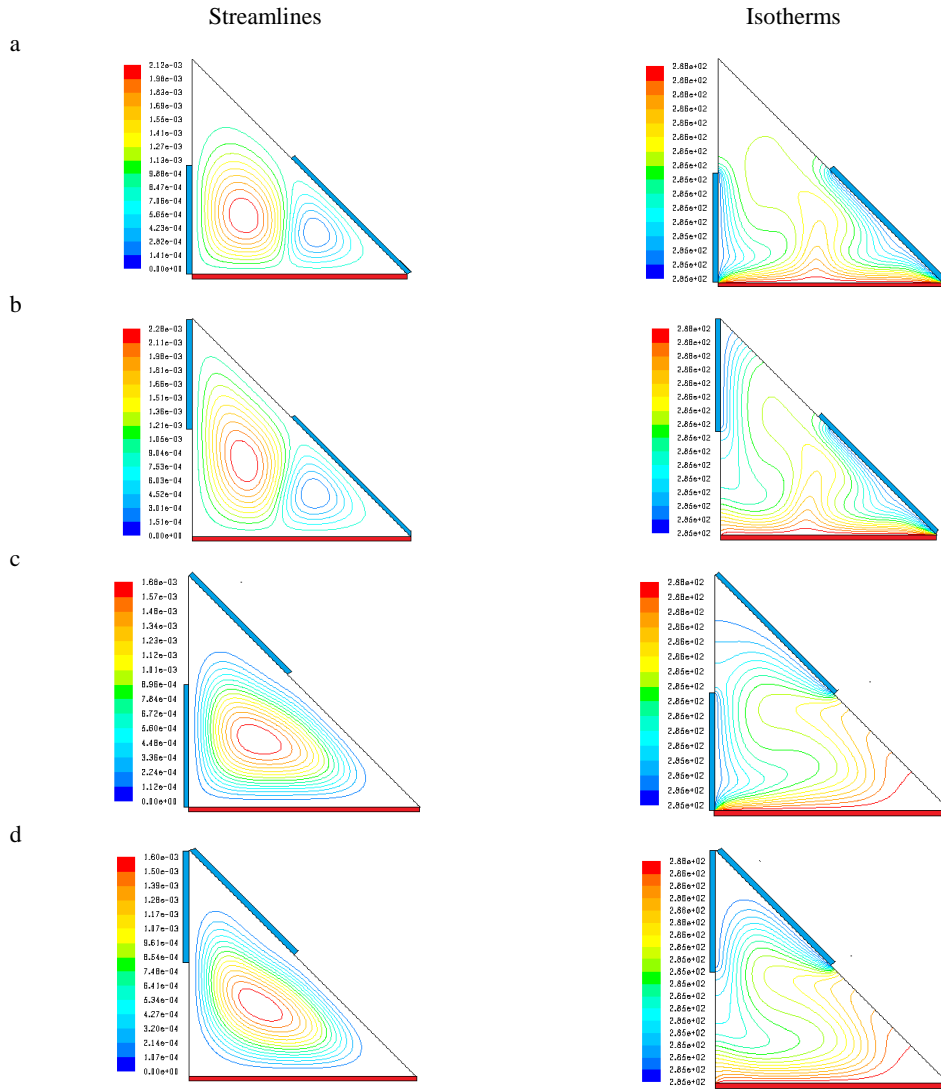


Fig. 6. Streamlines (left) and isotherms (right) at $\text{Ra} = 1 \times 10^5$ for a) case AB, b) case BC, c) case AD and d) case CD.

Yesiloz and Aydin(2013), shown in Figs. 3 & 4, by considering the same boundary conditions at $\text{Ra} = 10^5$ and $\text{Ra} = 5 \times 10^5$ for right-angled triangular enclosure filled with water.

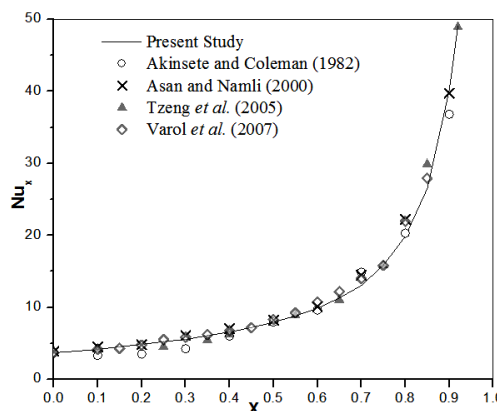


Fig. 5. Comparison of local Nusselt number with distance between the present work and the other published results for a triangular cavity.

Also, the variation in local Nusselt number with the position for triangular cavity is validated with the published data which displayed in Fig. 5. Both the results are showing quite good agreement with the published results.

The results of this present work computed through numerical simulation for a right-angled triangular cavity to demonstrate the influence of the physical parameters such as cold walls' configurations and Rayleigh number on streamline and isotherms contours as well as local and average Nusselt number which are shown in Figs. 6-10.

4. Results and discussions

4.1 Flow Structure and Isotherms

4.1.1 Effect of Different Configurations of Cold Walls

The effect of different positions of cold walls on streamlines and isotherms at $\text{Ra} = 1 \times 10^5$ are displayed in Fig.6a-d. In position AB, two

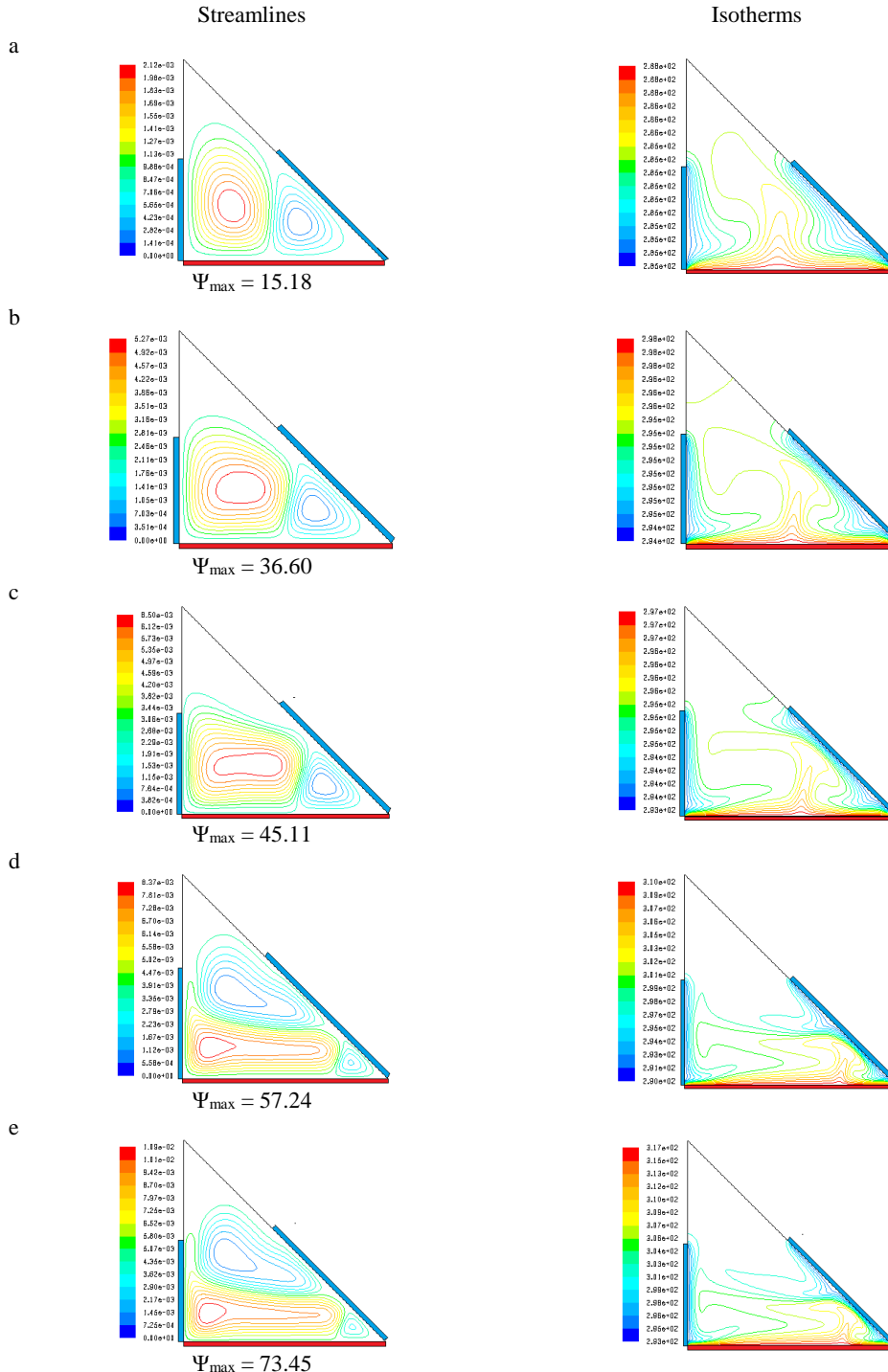


Fig. 7. Streamlines (left-hand) and isotherms (right-hand) intended for case AB at a) $\text{Ra} = 1 \times 10^5$, b) $\text{Ra} = 5 \times 10^5$, c) $\text{Ra} = 1 \times 10^6$, d) $\text{Ra} = 5 \times 10^6$ and e) $\text{Ra} = 1 \times 10^7$.

asymmetric vortices are formed; the primary cell occupied the most of the enclosure's space and rotates in counter clockwise direction adjacent to the side wall while the secondary cell was rotating clockwise near the inclined wall. The formation of large cell near the left wall signifies high flow intensity which leads the convection current. While near the inclined wall, some part of the fluid gets trapped and become stagnant due to the narrowness. This restricts the flow circulation (hydrodynamically inactive) and thus the heat

transfer is taking place by conduction only. Same phenomena occurs for the position BC except the primary cell which gets elongated towards the upper end of the cavity due to the change in position of the side cold wall. The elongation of the cell indicates the fluid particles carry a long path for heat transportation. In the third and fourth cases, shown in Figs. 6c&d, formation of single cell streamlines depicts the slow motion of fluid circulation and corresponding heat transfer rate. The isotherms are suppressed towards the cold walls in

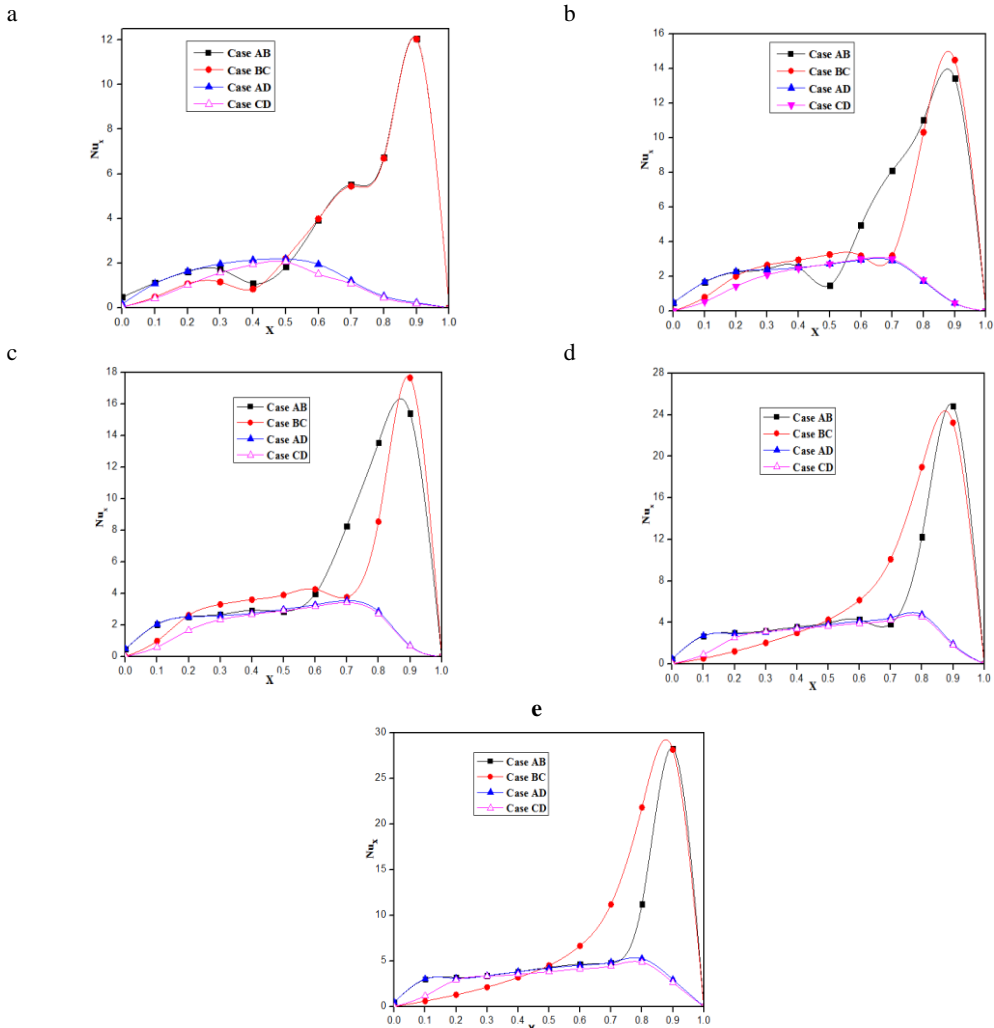


Fig. 8. Variation in local nusselt number for different position of cold wall at a) $Ra = 1 \times 10^5$, b) $Ra = 5 \times 10^5$, c) $Ra = 1 \times 10^6$, d) $Ra = 5 \times 10^6$ and e) $Ra = 1 \times 10^7$.

case of AB while in the remaining cases, it spreads throughout the cavity.

4.1.2 Effect of Rayleigh Number

Fig. 7a-e presented for the single case AB to demonstrate the effect of Rayleigh numbers on fluid flow and temperature distribution. At $Ra = 1 \times 10^5$, the flow circulation splits into two asymmetric cells which circulated near the side and inclined cold walls. The vortex structure of the cell is circular at the center, but it turns to an elliptic shape as the Ra increases to 10^6 . However, as the Rayleigh number increases more than 10^6 , the vortices are divided into three cells. The separation and deviation in the structure of the vortex with increasing Rayleigh number signify the penetration and elongation of the vortex between the hot and cold walls. This means, the flow strength is getting augmented with the increase of Rayleigh number which is responsible for the increment in convective heat transfer coefficient. The intensity of flow is clearly shown in Fig. 7a-e through stream functions. The maximum value of non-dimensional stream function are calculated as $\Psi_{\max} = 73.45$ for $Ra = 1 \times 10^7$. Correspondingly, at low Rayleigh number the

isotherms are distributed towards the cold walls and found less intense. But, as the Ra increases the thermal plumes are getting more intense and suppressed to the cold walls. At high Ra, the isotherms get stick to the cold walls. The increment in Rayleigh number augments the convection regime which leads to the enhancement of the heat transfer rate.

4.2 Local and Average Nusselt number

Fig. 8a-e illustrates the variation of local heat transfer rate (Nu_x) for bottom wall vs distance for various cooling positions at different Rayleigh number. The maximum local heat transfer rate ($Nu_x = 28.3$) has been obtained near the inclined cold wall because of the constriction at the bottom right corner of the cavity where both convection and conduction heat transfer are functioning. The high value of local Nusselt number is computed for positions AB and BC while low heat transfer rate ($Nu_x < 5$) has been observed for cold walls positions AD and CD for all Rayleigh numbers.

Fig. 9 demonstrates the variation of average nusselt number (Nu) with Ra for different configurations of

cold walls. It is interesting to note that the heat transfer rate increases with the increase of Rayleigh number. The heat transfer rate is obtained high for case AB and BC because of the direct contact of the isothermal hot wall with the cold walls. In case of AD, one side of the cold wall is in direct contact with the hot wall but due to counter-clockwise flow circulation and position of the cold walls, the hot molecules diffuse the heat to the adjacent molecules at low temperature before coming in contact with the cold walls. The same phenomenon occurs in case of CD. The heat transfer rates are less for the case AD and CD compare to AB and BC, because the upward moving hot fluid is carrying the less heat. The highest value of average Nusselt number is observed for the case AB ($\text{Nu} = 29.33$) and lowest for the position CD ($\text{Nu} = 12.23$) for $\text{Ra} = 1 \times 10^7$.

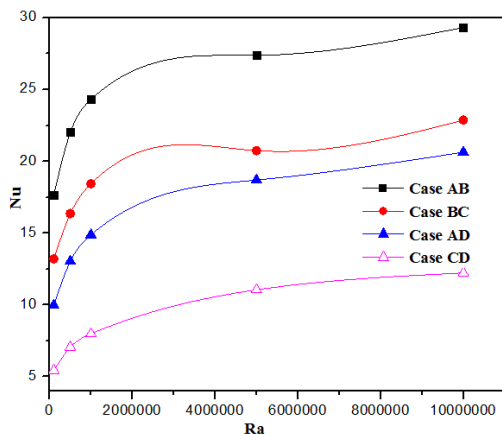


Fig. 9. Variation in average Nusselt number for different Rayleigh number and position of cold walls.

5. CONCLUSION

A numerical study has been performed in a triangular cavity filled with water for different positions of cold walls and for variant Rayleigh number. The results are validated qualitatively with the published experimental and numerical results by Yesiloz and Aydin (2013) and quantitatively by Akinsete and Coleman (1982), Asan and Namli (2000), Tzeng *et al.* (2005) and Varol *et al.* (2007). The analysis has been conducted for $\text{Ra} = 10^5-10^7$. Fluid flow and temperature distributions have been presented by streamlines and isotherms as well as the heat transfer rate is calculated in term of local and average Nusselt number. Based on the present investigation following observations have been made:

1. The values of streamfunction (flow strength) and the heat transfer rate increases with the increase of Rayleigh number.
2. Both, fluid flow and temperature fields are affected by the configurations of cold walls.
3. The heat transfer rate is high for the case AB compared to all other cases and low heat transfer rate is observed for the case CD which is shown in Fig. 10.
4. For medium heat transfer rate BC position could be preferred.

ACKNOWLEDGEMENT

The authors are very grateful to the reviewers for their precious and productive comments which have been utilized to improve the quality of this manuscript.

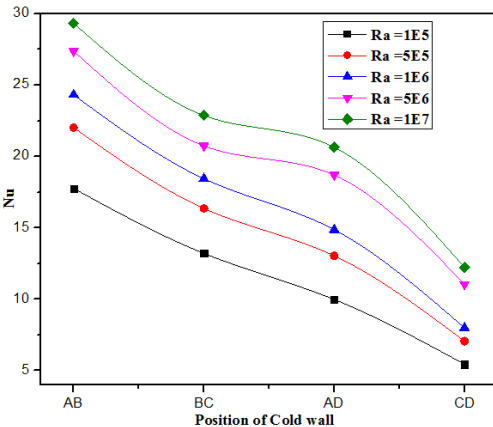


Fig. 10. Variation in average Nusselt number at different cold walls positions for different Rayleigh number.

REFERENCE

- Akinsete, V. A. and T. A. Coleman (1982). Heat transfer by steady laminar free convection in triangular enclosures. *International Journal of Heat and Mass Transfer* 25(7), 991 – 998.
- Asan, H. and L. Namli (2000). Laminar natural convection in a pitched roof of triangular cross-section: summer day boundary conditions. *Energy and Buildings* 33(1), 69 – 73.
- Basak, T., G. Aravind and S. Roy (2009). Visualization of heat flow due to natural convection within triangular cavities using bejan'sheatline concept. *Int. J. Heat Mass Transfer* 52, 2824-2833.
- Basak, T., P. Gunda and R. Anandalakshmi (2012). Analysis of entropy generation during natural convection in porous right-angled triangular cavities with various thermal boundary conditions. *Int. J. Heat Mass Transfer* 55, 4521-4535.
- Bhardwaj, S. and A. Dalal (2013). Analysis of natural convection heat transfer and entropy generation inside right-angled triangular enclosure. *Int. J. Heat Mass transfer* 65, 500-513.
- Bose, P. K., D. Sen, R. Panua and A. K. Das (2013). Numerical analysis of laminar natural convection with a solid adiabatic fin attached to the hot vertical wall. *Journal of Applied Fluid Mechanics* 6(4), 501-510.
- Flack, R. D., T. T. Konopnicki and J. H. Rooke (1979). The measurement of natural convective

- heat transfer in triangular enclosures. *J. Heat Transfer* 101, 770-772.
- Flack, R. D. (1980). The experimental measurement of natural convection heat transfer in triangular enclosures heated or cooled from below. *J. Heat Transfer* 102, 770-772.
- Fluent User's Guide, Release 6.3.26, Fluent Incorporated (2005-01-06).
- Kaluri, R. S., R. Anandalakshmi and T. Basak (2010). Bejan'sheatline analysis of natural convection in right-angled triangular enclosures: effects of aspect-ratio and thermal boundary conditions. *Int. J. Thermal Sciences* 49, 1576-1592.
- Kent, E. F. (2009). Numerical analysis of laminar natural convection in isosceles triangular enclosures for cold base and hot inclined walls. *Mechanics Research Communication* 36, 497-508.
- Koca, A., H. F. Oztop and Y. Varol (2007). The effects of prandtl number on natural convection in triangular enclosures with localized heating from below. *Int. Communication Heat Mass Transfer* 34, 511-519.
- Pullepu, B. and A. J. Chamkha (2013). Numerical solutionof unsteady laminar free convection from a vertical cone with non-uniform surface heat flux. *Journal of Applied Fluid Mechanics* 6(3), 357-367.
- Rahman, M. M., H. F.Oztop, A. Ahsan and J. Orfi (2012). Natural convection effects on heat and mass transfer in a curvilinear triangular cavity. *Int. J. Heat Mass Transfer* 55, 6250-6259.
- Ridouane, E. I., A. Campo and J. Y. Chang (2005). Natural convection patterns in right-angled triangular cavities with heated vertical sides and cooled hypotenuses. *Journal of heat transfer* 127, 1181- 1186.
- Saha, S. C. (2011). Unsteady natural convection in a triangular enclosure under isothermal heating. *Energy Buildings* 43, 695-703.
- Tzeng, S. C., J. H. Liou and R. Y. Jou (2005). Numerical simulation-aided parametric analysis of natural convection in a roof of triangular enclosures. *Heat Transfer Engineering* 26, 69 – 79.
- Varol, Y., H. F. Oztop, M. Mobedi and I. Pop (2007). Visualization of natural convection heat transport using heatline method in porous non-isothermally heated triangular cavity. *Int. J. Heat Mass Transfer* 51, 5040-5051.
- Varol, Y., H. F.Oztop and T. Yilmaz (2007). Natural convection in triangular enclosures with protruding isothermal heater. *Int. J. Heat Mass Transfer* 50, 2451-2462.
- Varol, Y., H. F.Oztop and A. Varol (2008). Effects of thin fin on natural convection in porous triangular enclosures. *Int. J. Thermal Science* 46, 1033-1045.
- Varol, Y., H. F.Oztop and A. Koca(2008). Entropy production due to free convection in partially heated isosceles triangular enclosures. *Applied Thermal Engineering* 28, 1502-1513.
- Walid, A. and O. Ahmed (2012). Buoyancy induced heat transfer and fluid flow inside a prismatic cavity. *Journal of Applied Fluid mechanics* 3(2), 77-86.
- Xu, X., Z. Yu, Y. Hu, L. Fan and K. Cen(2010). A numerical study of laminar natural convection heat transfer around a horizontal cylinder inside a concentric air-filled triangular enclosure. *Int. J. Heat Mass Transfer* 53, 345-355.
- Yesiloz, G. and O. Aydin (2013). Laminar natural convection in right-angled triangular enclosures heated and cooled on adjacent walls. *Int. J. Heat Mass Transfer* 60, 365-374.